Dual-phase-lag model on microelongated thermoelastic rotating medium

Mohamed I. A. Othman[1], Sarhan Y. Atwa[2], E. E. M. Eraki[3], Mohamed F. Ismail[4]
[1, 3]Department of Mathematics, Faculty of Science, Zagazig University, P.O. Box 44519, Zagazig, Egypt
[2, 4]Department of Engineering Mathematics and Physics, Higher Institute of Engineering,
El Shorouk Academy, P.O. Box 11837, Cairo, Egypt
[1]Corresponding author
E-mail: [1]*m_i_a_othman@yahoo.com*, [2]*srhan_1@yahoo.com*, [3]*ebtesam.eraki@yahoo.com*,
[4]*m.fekry2015@yahoo.com*

Received 17 April 2022; accepted 12 May 2022
DOI https://doi.org/10.21595/jets.2022.22597

Abstract. The dual-phase-lag (DPL) model is applied to study the influence of rotation on a two-dimensional micro-elongated thermoelastic medium problem. Mechanical force along with the layer of the elastic half-space interface and micro-elongated thermoelastic half-space is applied. The analytic expressions for displacement component, temperature distribution, micro-elongational scalar and stress components have been derived and represented graphically. The rotation has been studied in the presence DPL model and Lord-Shulman theory.

Keywords: thermoelasticity, micro-elongation, rotation, normal mode, elastic solid.

Nomenclature

σ_{ij}	Component of stress tensor for micro-elongated medium
ρ	Density in micro-elongated medium
u	Displacement vector in micro-elongated medium
Ω	Angular velocity
a_0, λ_0, λ_1	Micro-elongational constants
α_{t_1}, α_{t_2}	Coefficient of linear thermal expansion where $\beta_0 = (3\lambda + 2\mu)\alpha_{t_1}$, $\beta_1 = (3\lambda + 2\mu)\alpha_{t_2}$
j_0	Microinertia
φ	Micro-elongational scalar
T	Absolute temperature
T_0	Reference temperature
k	Thermal conductivity in micro-elongated medium
c_e	Specific heat at constant strain in micro-elongated medium
τ_θ	Temperature gradient parameter
τ_q	Heat flux parameter
λ, μ	Lame's constants in micro-elongated medium
u^e	Displacement vector in elastic medium
ρ^e	Density in elastic medium
λ^e, μ^e	Lame's constants in elastic medium
k^e	Thermal conductivity in elastic medium
c_e^e	Specific heat at constant strain in elastic medium

1. Introduction

A microelongated elastic solid possesses four degrees of freedom: three for translation and micro-elongation. In micro-elongation theory, the material particles can perform only volumetric micro-elongation in addition to classical deformation of the medium. The material points of such a medium can stretch and contract independently of their translations. Solid-liquid crystals,

composite materials reinforced with chopped elastic fibres porous media with pores filled with non-viscous fluid or gas can be categorized as micro-elongated medium. The variation of periodical heat source response in a functionally graded micro-elongated medium was discussed by [1, 2]. The plane strain problem in a thermoelastic micro-elongated solid with an overlying infinite non-viscous fluid was discussed by [3]. More interesting problems have been studied about the thermoelastic micro-elongated solid in different cases [4-9].

In the generalized theories, the governing equations involve thermal relaxation times and they are of a hyperbolic type. The extended thermoelasticity theory by [10-14] which introduces one relaxation time in the thermoelastic process and the temperature-rate dependent theory of thermoelasticity by [15], which takes into account two relaxation times are two well-established generalized theories of thermoelasticity.

A new model called the dual-phase-lag model for the heat transport mechanism in which Fourier's law is replaced by an approximation to the modification of Fourier's law with two different time translations for the heat flux and the temperature gradient was investigated by [16-20]. The effect of thermal loading due to laser pulse in generalized thermoelastic medium with voids in the dual-phase-lag model was studied by [21]. A dynamic problem in thermoelastic solid using a dual-phase-lag model with an internal heat source was explained by [22]. The effect of rotation on micropolar generalized thermoelasticity with two-temperatures and the thermal laser pulse using a DPL model has been discussed by [23, 24].

In this paper, the effect of rotation on a two-dimensional micro-elongated thermoelastic medium problem has been discussed. The normal mode analysis is used to derive the expressions for the considered variables for a DPL model of thermoelasticity and the variances of the considered variables are represented graphically.

2. Formulation of the problem

The system of prevailing equations of a microelongated thermoelastic solid with rotation, in the DPL model, as [4, 7] (Fig. 1):

$$\sigma_{ij,j} = \rho\,[u_{i,tt} + \{\Omega \times (\Omega \times u)\}_i + (2\Omega \times u_{,t})_i], \tag{1}$$

$$a_0\,\varphi_{,ii} + \beta_1 T - \lambda_1 \varphi - \lambda_0 u_{j,j} = \frac{1}{2}\rho j_0\,\varphi_{,tt}, \tag{2}$$

$$k\left(1 + \tau_\theta \frac{\partial}{\partial t}\right) T_{,ii} = \left(1 + \tau_q \frac{\partial}{\partial t}\right)\left(\rho\, c_e \frac{\partial T}{\partial t} + \beta_0 T u_{k,kt}\right) + \beta_1 T_0 \varphi_{,t}, \tag{3}$$

$$\sigma_{ij} = 2\,\mu\,\varepsilon_{ij} + (\lambda\, e - \beta_0\, T + \lambda_0\,\varphi)\,\delta_{ij}. \tag{4}$$

where the displacement vector $u\,(x, z, t) = u\,(u_1, 0, u_3)$, and the rotation $\Omega = (0, \Omega, 0)$ then the equations of motion are given by:

$$\mu\,\nabla^2 u_1 + (\lambda + \mu) e_{,x} - \beta_0\, T_{,x} + \lambda_0 \varphi_{,x} = \rho\,(u_{1,tt} - \Omega^2 u_1 + 2\Omega u_{3,t}), \tag{5}$$

$$\mu\,\nabla^2 u_3 + (\lambda + \mu) e_{,z} - \beta_0\, T_{,z} + \lambda_0 \varphi_{,z} = \rho\,(u_{3,tt} - \Omega^2 u_3 + 2\Omega u_{1,t}). \tag{6}$$

For simplification, we shall use the following non-dimensional variables:

$$x'_i = \frac{w^*}{c_1}\,x_i, \quad z' = \frac{w^*}{c_1}\,z, \quad u'_i = \frac{w^*\,\rho\,c_1}{\beta_0\,T_0}\,u_i, \quad u_i^{e\prime} = \frac{w^*\,\rho\,c_1}{\beta_0\,T_0}\,u_i^e,$$

$$t' = w^*\,t, \quad \tau'_\theta = w^*\,\tau_\theta, \quad \tau'_q = w^*\,\tau_q, \quad \sigma'_{ij} = \frac{\sigma_{ij}}{\beta_0\,T_0}, \quad \sigma_{ij}^{e\prime} = \frac{\sigma_{ij}^e}{\beta_0\,T_0}, \tag{7}$$

$$\varphi' = \frac{\lambda_0}{\beta_0\,T_0}\varphi, \quad T' = \frac{T}{T_0}, \quad \Omega' = \frac{\Omega}{w^*}, \quad P'_1 = \frac{P_1}{\beta_0\,T_0}, \quad w^* = \frac{\rho\,c_1^2\,c_e}{k}, \quad c_1^2 = \frac{\lambda + 2\,\mu}{\rho}.$$

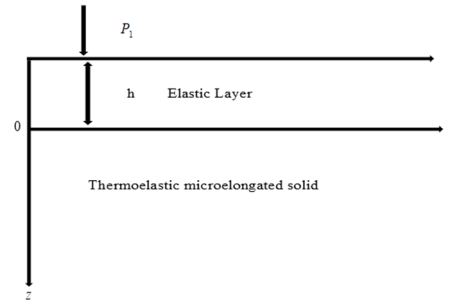

Fig. 1. Geometry of the problem

The displacement potentials $\Phi(x,z,t)$ and $\Psi(x,z,t)$ which relate to displacement components have been introduced, we obtain:

$$u_1 = \Phi_{,x} + \psi_{,z}, \quad u_3 = \Phi_{,z} - \psi_{,x}. \tag{8}$$

From Eqs. (7) and (8) into Eqs. (2), (3), (5) and (6), we obtain:

$$\left[(a_1 + a_2)\,\nabla^2 + \Omega^2 - \frac{\partial^2}{\partial t^2}\right]\Phi + 2\Omega\psi_{,t} - T + \varphi = 0, \tag{9}$$

$$-2\Omega\Phi_{,t} + \left(a_1\nabla^2 + \Omega^2 - \frac{\partial^2}{\partial t^2}\right)\psi = 0, \tag{10}$$

$$-a_5\nabla^2\Phi + a_3 T + \left(\nabla^2 - a_4 - a_6\frac{\partial^2}{\partial t^2}\right)\varphi = 0, \tag{11}$$

$$-a_8\left(1 + \tau_q\,\frac{\partial}{\partial t}\right)\nabla^2\Phi_{,t} + \left(1 + \tau_\theta\frac{\partial}{\partial t}\right)\nabla^2 T - a_7\left(1 + \tau_q\frac{\partial}{\partial t}\right)T_{,t} - a_9\varphi = 0. \tag{12}$$

3. Normal mode analysis

The solution of the considered physical variable can be decomposed in terms of normal modes as the following form:

$$\left[\,u_i, \varphi, T, \psi, \Phi, \sigma_{ij}, u_i^e, \sigma_{ij}^e\,\right](x,z,t) = \left[\,u_i^*, \varphi^*, T^*, \psi^*, \Phi^*, \sigma_{ij}^*, u_i^{e*}, \sigma_{ij}^{e*}\,\right](z)e^{(\omega\, t + i\, b\, x)}, \tag{13}$$

where, ω is a complex constant, $i = \sqrt{-1}$, b is the wave number in the x direction.

Using Eq. (13) into Eqs. (9)-(12), then we have:

$$(a_{10}D^2 + a_{11})\,\Phi^* + 2\Omega\omega\psi^* - T^* + \varphi^* = 0, \tag{14}$$
$$-2\Omega\omega\Phi^* + (a_1 D^2 + a_{12})\,\psi^* = 0, \tag{15}$$
$$(-a_5 D^2 + a_{13})\Phi^* + a_3 T^* + (D^2 - a_{14})\varphi^* = 0, \tag{16}$$
$$(-a_{17}D^2 + a_{18})\Phi^* + (a_{16}D^2 - a_{19})\,T^* - a_9 w\varphi^* = 0. \tag{17}$$

Eqs. (14-17) have a non-trivial solution if the determinant coefficients of the physical quantities equal to zero, then we get:

$$(D^8 - AD^6 + BD^4 - CD^2 + E)\,\{\Phi^*(z)\,, \psi^*(z)\,, T^*(z)\,, \varphi^*(z)\} = 0. \tag{18}$$

The coefficients a_i, A, B, C, E and H_{in} are given in Appendix A1.

Eq. (18) can be factorized as:

$$(D^2 - k_1^2)(D^2 - k_2^2)(D^2 - k_3^2)(D^2 - k_4^2)\{\Phi^*(z)\,, \psi^*(z), T^*(z), \varphi^*(z)\} = 0, \tag{19}$$

where, k_n^2, $(n = 1, 2, 3, 4)$ are roots of the characteristic equation of Eq. (19).

The general solutions of Eq. (19) bound as $(z \to \infty)$ is given by:

$$(\Phi^*, \psi^*, T^*, \varphi^*)(z) = \sum_{n=1}^{4} (1, H_{1n}, H_{2n}, H_{3n})\, M_n e^{-k_n z}. \tag{20}$$

Substituting from Eq. (20) into Eq. (8) we obtain the components of displacements:

$$u_1^*(z) = \sum_{n=1}^{4} (ib - k_n H_{1n}) M_n e^{-k_n z}, \tag{21}$$

$$u_3^*(z) = \sum_{n=1}^{4} -(k_n + ibH_{1n}) M_n e^{-k_n z}. \tag{22}$$

Substituting Eqs. (7) and (13) into (4) and by using of Eqs. (20)-(22) we get:

$$(\sigma_{xx}^*, \sigma_{zz}^*, \sigma_{xz}^*)(z) = \sum_{n=1}^{4} (H_{4n}, H_{5n}, H_{6n}) M_n e^{-k_n z}. \tag{23}$$

The equations of motion and stress components in an elastic medium are given by [7]:

$$\sigma_{ij,j}^e = \rho^e\, u_{i,tt}^e, \tag{24}$$

$$\sigma_{ij}^e = \lambda^e u_{k,k}^e \delta_{ij} + \mu^e\, (u_{i,j}^e + u_{j,i}^e). \tag{25}$$

Substituting from Eqs. (7) and (13) into Eq. (24):

$$(l_3 D^2 - \delta_1) u_1^{e*} + i\, b\, l_2 D\, u_3^{e*} = 0, \tag{26}$$

$$ibl_2 D u_1^{e*} + (l_1 D^2 - \delta_2)\, u_3^{e*} = 0. \tag{27}$$

Eliminating u_1^{e*}, u_3^{e*} between Eqs. (26) and (27), we obtain:

$$(D^4 - GD^2 + N)\{u_1^{e*}(z), u_3^{e*}(z)\} = 0. \tag{28}$$

Eq. (28) can be factorized as:

$$(D^2 - r_1^2)(D^2 - r_2^2)\{u_1^{e*}(z), u_3^{e*}(z)\} = 0, \tag{29}$$

where, r_n^2, $(n = 1, 2)$ are the roots of the characteristic equation of Eq. (29), the solutions of Eq. (29) are:

$$u_1^{e*}(z) = \sum_{n=1}^{2} R_n\, e^{-r_n z} + \sum_{n=1}^{2} R_{n+2}\, e^{r_n z}, \tag{30}$$

$$u_3^{e*}(z) = \sum_{n=1}^{2} L_{1n}\, R_n\, e^{-r_n z} + \sum_{n=1}^{2} L_{1(n+2)}\, R_{n+2}\, e^{r_n z}. \tag{31}$$

From Eqs. (7) and (13) into (25) and by using the Eqs. (30) and (31), we obtain the components of stresses in an elastic medium:

$$\sigma_{xx}^{e*}(z) = \sum_{n=1}^{2} L_{2n}\, R_n\, e^{-r_n z} + \sum_{n=1}^{2} L_{2(n+2)}\, R_{n+2}\, e^{r_n z}, \tag{32}$$

$$\sigma_{zz}^{e*}(z) = \sum_{n=1}^{2} L_{3n}\, R_n\, e^{-r_n z} + \sum_{n=1}^{2} L_{2(n+2)}\, R_{n+2}\, e^{r_n z}, \tag{33}$$

$$\sigma_{xz}^{e*}(z) = \sum_{n=1}^{2} L_{4n}\, R_n\, e^{-r_n z} + \sum_{n=1}^{2} L_{4(n+2)}\, R_{n+2}\, e^{r_n z}, \tag{34}$$

where, the coefficients l_i, δ_i, G, N and L_{in} are given in Appendix A2

4. The boundary conditions

The parameters M_n, ($n = 1, 2, 3, 4$) and R_n, ($n = 1, 2, 3, 4$) can be determined by using the boundary conditions at the surface are [3-7]:

$$\begin{aligned} &\sigma_{zz} = \sigma_{zz}^{e}, \quad \sigma_{xz} = \sigma_{xz}^{e}, \quad u_1 = u_1^{e}, \quad u_3 = u_3^{e}, \quad \varphi = 0, \quad \frac{\partial T}{\partial z} = 0, \quad \text{at} \quad z = 0, \\ &\sigma_{zz} = \sigma_{zz}^{e} - P_1\, e^{(\omega t + i b x)}, \quad \sigma_{xz} = 0, \quad \text{at} \quad z = -h, \end{aligned} \tag{35}$$

where, P_1 is the magnitude of the mechanical force.

The using of the expressions of the variables considered in the past boundary conditions Eq. (35), to get the equations that are satisfied with the parameters. And hence, eight equations will be gained. The inverse matrix method is applied to the eighth equation, to obtain the value of M_n ($n = 1, 2, 3, 4$) and R_n ($n = 1, 2, 3, 4$):

$$\begin{pmatrix} M_1 \\ M_2 \\ M_3 \\ M_4 \\ R_1 \\ R_2 \\ R_3 \\ R_4 \end{pmatrix} = \begin{pmatrix} H_{51} & H_{52} & H_{53} & H_{54} & -L_{31} & -L_{32} & -L_{33} & -L_{34} \\ H_{61} & H_{62} & H_{63} & H_{64} & -L_{41} & -L_{42} & -L_{43} & -L_{44} \\ ib - k_1 H_{11} & ib - k_2 H_{12} & ib - k_3 H_{13} & ib - k_4 H_{14} & -1 & -1 & -1 & -1 \\ -k_1 - ibH_{11} & -k_2 - ibH_{12} & -k_3 - ibH_{13} & -k_4 - ibH_{14} & -L_{11} & -L_{12} & -L_{13} & -L_{14} \\ H_{31} & H_{32} & H_{33} & H_{34} & 0 & 0 & 0 & 0 \\ -k_1 H_{21} & -k_2 H_{22} & -k_3 H_{23} & -k_4 H_{24} & 0 & 0 & 0 & 0 \\ H_{51} e^{k_1 h} & H_{52} e^{k_2 h} & H_{53} e^{k_3 h} & H_{54} e^{k_4 h} & -L_{31} e^{r_1 h} & -L_{32} e^{r_2 h} & -L_{33} e^{-r_1 h} & -L_{34} e^{-r_2 h} \\ H_{61} e^{k_1 h} & H_{62} e^{k_2 h} & H_{63} e^{k_3 h} & H_{64} e^{k_4 h} & 0 & 0 & 0 & 0 \end{pmatrix}^{-1} \begin{pmatrix} 0 \\ 0 \\ 0 \\ 0 \\ 0 \\ 0 \\ -P_1 \\ 0 \end{pmatrix}. \tag{36}$$

5. Numerical results and discussion

The analysis is conducted for aluminum epoxy-like material as [24]: $\lambda = 7.59\times10^{10}$ N/m^2, $\mu = 1.89\times\times10^{10}$ N/m^2, $a_0 = 0.61\times10^{-10}$ N, $\rho = 2.19\times10^{3}$ kg/m^3, $\beta_0 = \beta_1 = 0{,}05\times10^{5}$ N/(m^2.k), $c_e = 966$ J/(kg.k), $k = 252$ J/(m.s.k), $j_0 = 0.196\times10^{-4}$ m^2, $\lambda_0 = \lambda_1 = 0.37\times10^{10}$ N/m^2, $T_0 = 293$ k, $\tau_\theta = 0.02$ s, $\tau_q = 0.5$ s, $\omega = \omega_0 + i\zeta$, $\omega_0 = 3.56$, $\zeta = -4.81$, $b = 8$, $h = 1\times10^{-6}$.

The physical constants for elastic medium (granite) as [5]: $\lambda^e = 0.884\times10^{10}$ N/m^2, $\mu^e = 1.2667\times10^{10}$ N/m^2, $\rho^e = 2.6\times10^{3}$ kg/m^3, $c_e^e = 720.7$ J/(kg.k), $k^e = 3.1$ J/(m.s.k.)

In light of the results of this paper, the computations are conducted for the value of non-dimensional time $t = 0.01$, in the range of $0 \le z \le 0.4$ on the surface $x = 3.01$. The numerical strategy stated herein is utilized for the distribution of horizontal displacement u_1, the vertical displacement u_3, the temperature T, the micro-elongational scalar φ, the stress components σ_{xx}, σ_{zz} and σ_{xz} with distance z. To study the influence of rotation on the solution in the DPL model and the L-S theory and the effect of phase-lag of heat flux and phase-lag of temperature gradient on the solution in the DPL model, this paper introduces the results of the numerical assessment in the form of graphs. The results are shown in Figs. 2-15 for the mechanical force with magnitude $P_1 = 1$ for the DPL model and the L-S theory.

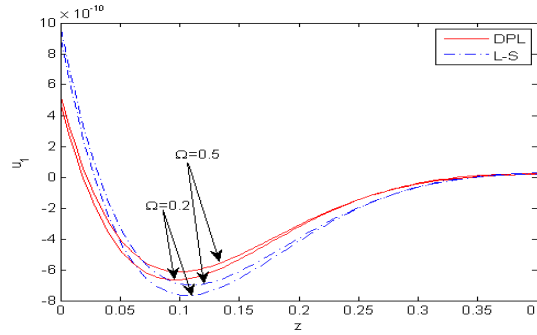

Fig. 2. Distribution of the horizontal displacement u_1 with the distance z

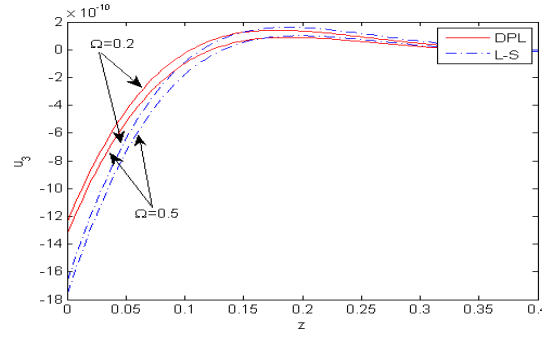

Fig. 3. Distribution of the vertical displacement u_3 with the distance z

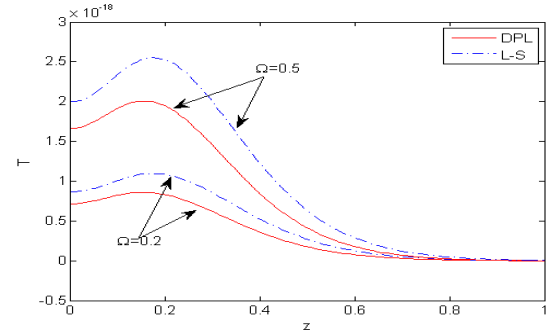

Fig. 4. Distribution of the temperature T with distance z

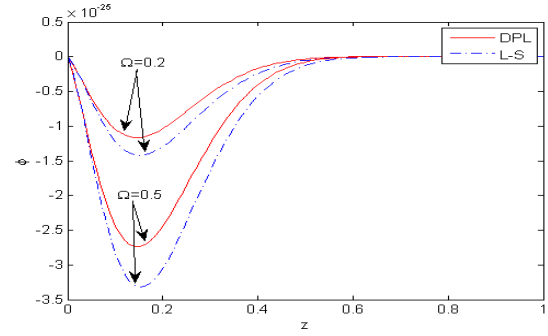

Fig. 5. Distribution of the micro-elongational scalar φ with the distance z

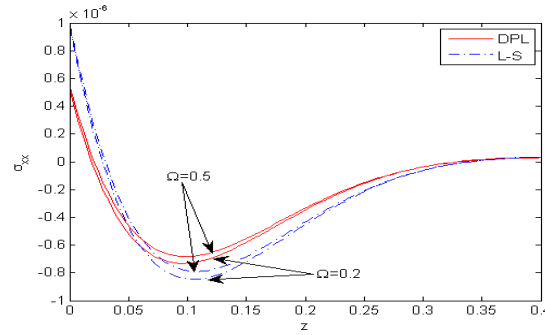

Fig. 6. Distribution of the force stress component σ_{xx} with the distance $\boldsymbol{z}$

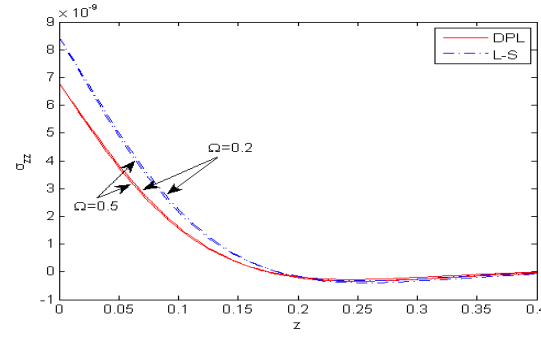

Fig. 7. Distribution of the force stress component σ_{zz} with the distance $\boldsymbol{z}$

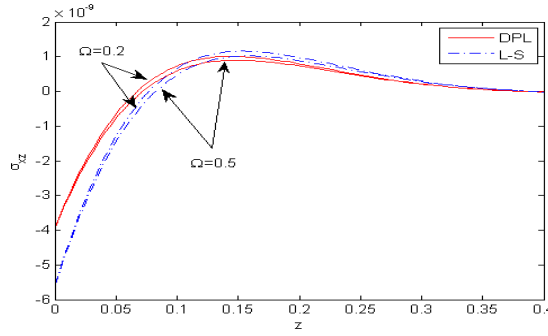

Fig. 8. Distribution of the force stress component σ_{xz} with horizontal distance $\boldsymbol{z}$

5.1. Influence of rotation

Figs. 2-8 show comparison between the displacement components u_1, u_3, the temperature T, the micro-elongational scalar φ and the force stresses components σ_{xx}, σ_{zz}, σ_{xz} for various values of Ω ($\Omega = 0.2, 0.5$) for the DPL model and the L-S theory. Fig. 2 represents the distribution of the horizontal displacement $u_1$with the distance z. It is observed that u_1 increases with the increase of rotation for the two theories. In the (DPL) model and the L-S theory, the values of the horizontal displacement u_1 for $\Omega = 0.2$ are small as opposed to those for $\Omega = 0.5$. Fig. 3 illustrates the variation of the vertical displacement u_3 against the distance z, it is observed that the effect of rotation Ω is inversely proportional to the value of the vertical displacement u_3 in the DPL model and the L-S theory i.e the rotation Ω has a decreasing effect. Fig. 4 describes the distribution of the temperature T with the distance z. In this figure, all curves start from a positive value and then converge to zero with large values of the distance z and fulfill the boundary condition. It is obvious

that the values of the temperature T increases with increase of rotation for the two theories. Fig. 5 shows the variation of the micro-elongational scalar φ against the distance z, it is clear that the values of φ start from zero and decrease to a minimum then increase up to vanish. It is obvious that the values of φ increase with the decrease of rotation for two theories, and satisfies the boundary condition. Fig. 6 is plotted to describe the distribution of the stress components σ_{xx} with the distance z. In this figure, all curves begin from a positive value, then decrease to a minimum and increase up to vanishes at large values of z. The effect of rotation Ω is directly proportional to the value of the stress component σ_{xx} in both the DPL model and the L-S theory. Fig. 7 exhibits the variation of the stress component σ_{zz} against the distance z. In the DPL model, the effect of different values of rotation is hardly visible. It is shown that the influence of rotation is inversely proportional to the value of the stress component σ_{zz} in the L-S theory. Fig. 8 compares among the two different values of rotation for the DPL model and the L-S theory. It is obvious that the value of the stress component σ_{xz} increases as the rotation decreasing.

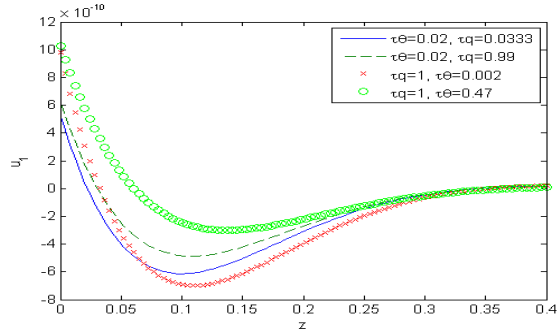

Fig. 9. Distribution of the horizontal displacement u_1 with the distance z

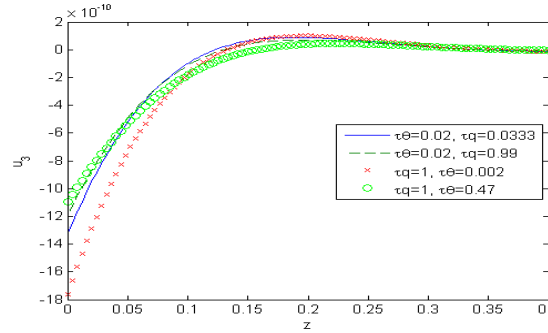

Fig. 10. Distribution of the vertical displacement u_3 with the distance z

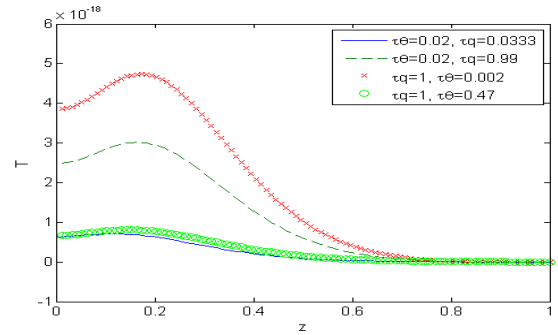

Fig. 11. Distribution of the temperature T with distance z

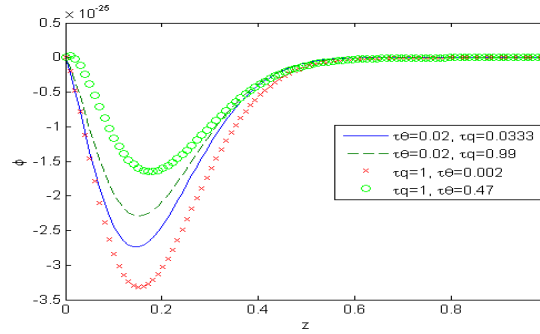

Fig. 12. Distribution of the micro-elongational scalar φ with the distance z

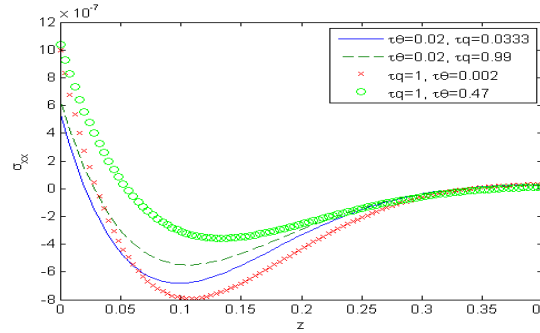

Fig. 13. Distribution of the force stress component σ_{xx} with the distance z

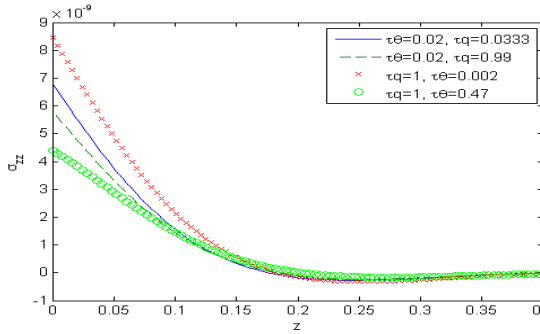

Fig. 14. Distribution of the force stress component σ_{zz} with the distance z

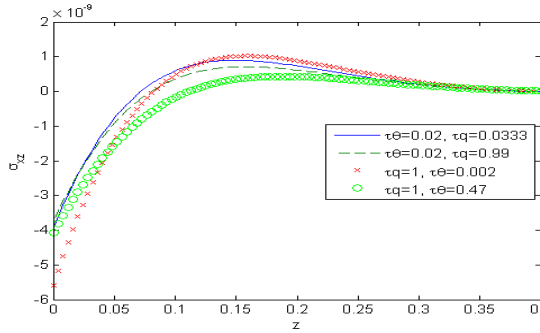

Fig. 15. Distribution of the force stress component σ_{xz} with the distance z

5.2. Influence of the phase-lag of the heat flux and the phase-lag of temperature gradient

Figs. 9-15 show comparison between the displacement components u_1, u_3, the temperature T, the micro-elongational scalar φ and the force stress components σ_{xx}, σ_{zz}, σ_{xz}, when it comes to thermoelasticity the DPL model for different values of the temperature gradient phase-lag τ_θ, such as $\tau_\theta = 0.002, 0.47$ at $\tau_q = 1$, $\Omega = 0.5$ and for different values of the heat flux phase-lag $\tau_q = 0.0333, 0.99$ at $\tau_\theta = 0.02$, $\Omega = 0.5$. Fig. 9 depicts that the phase-lag of temperature gradient and the heat flux have an increasing effect on the magnitude of the horizontal displacement u_1, whereas in fig. 15 they have a decreasing effect on the magnitude of the stress component σ_{xz} in the range $0.05 \leq z \leq 0.4$. Figs. 10 and 13 show that the phase-lag of the heat flux has an increasing effect on the vertical displacement u_3 over the range $0 \leq z \leq 0.11$ and on the stress component σ_{xx} over the range $0 \leq z \leq 0.4$, whereas, the phase-lag of the temperature gradient has a decreasing influence on both. Figs. 11 and 14 in that order, exhibit that the temperature T, and the stress component σ_{zz} are inversely proportional to the value of τ_q for $z > 0$. Fig. 12, explains that the value of micro-elongational scalar φ increases with the increase of τ_q and τ_θ.

5.3. The 3D surface curves

Figs. 16-21 are representing the 3D surface curves for the physical quantities, i.e., the horizontal displacement component u_3, the micro-elongational scalar φ and the stress components σ_{xx}, σ_{xz}, for the DPL model by keeping in mind the effect of rotation $\Omega = 0.5$. The importance of these figures is that they have been utilized to study the dependence of previous physical quantities on both components of distance.

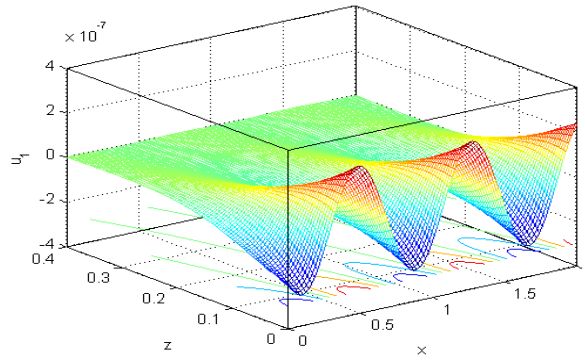

Fig. 16. 3D curve distribution of the horizontal displacement $u_1$versus distances at $\Omega = 0.5 \tau_\theta = 0.02$, $\tau_q = 0.5$

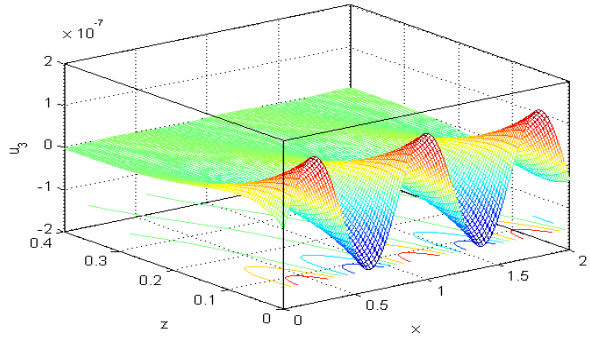

Fig. 17. 3D curve distribution of the vertical displacement u_3 versus distances at $\Omega = 0.5$, $\tau_\theta = 0.02$, $\tau_q = 0.5$

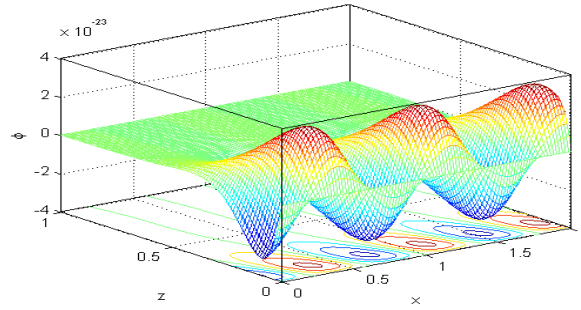

Fig. 18. 3D curve distribution of the micro-elongational scalar φ versus distances at $\Omega = 0.5$, $\tau_\theta = 0.02$, $\tau_q = 0.5$

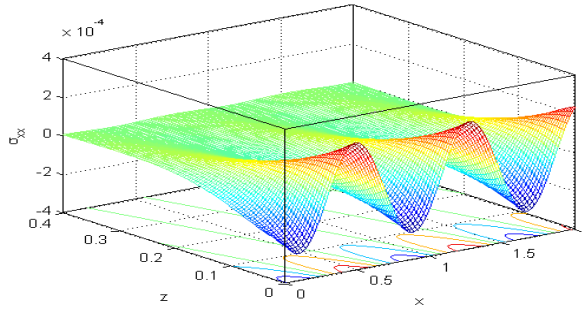

Fig. 19. 3D curve distribution of the force stress component σ_{xx} versus distances at $\Omega = 0.5$, $\tau_\theta = 0.02$, $\tau_q = 0.5$

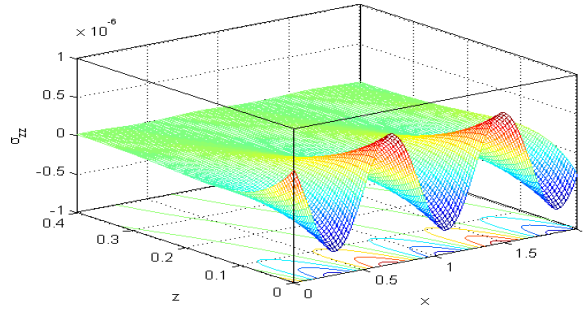

Fig. 20. 3D curve distribution of the force stress component σ_{zz} versus distances at $\Omega = 0.5$, $\tau_\theta = 0.02$, $\tau_q = 0.5$

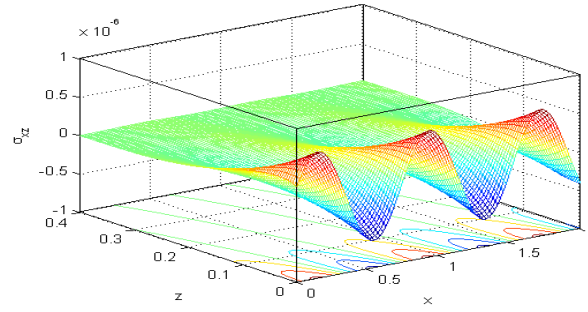

Fig. 21. 3D curve distribution of the force stress component σ_{xz} versus distances at $\Omega = 0.5$, $\tau_\theta = 0.02$, $\tau_q = 0.5$

6. Conclusions

According to the results of this work, one can see that the effect of rotation, the micro-elongational scalar and the applied boundary conditions play a major role in the study of thermoelastic medium deformation. The effect of rotation and the micro-elongational scalar has an obvious influence on all physical quantities. All the physical quantities, converge to zero very steeply with the distance z increases. A comparison between the DPL model and the L-S theory is conducted. An analytical solution depended on normal mode analysis of the problem on thermoelastic micro-elongated layer by encircling finite elastic under influence of the rotation has been developed and used it.

References

[1] S. Shaw and B. Mukhopadhyay, "Periodically varying heat source response in a functionally graded microelongated medium," *Applied Mathematics and Computation*, Vol. 218, No. 11, pp. 6304–6313, Feb. 2012, https://doi.org/10.1016/j.amc.2011.11.109

[2] S. Shaw and B. Mukhopadhyay, "Moving Heat Source Response in a Thermoelastic Microelongated Solid," *Journal of Engineering Physics and Thermophysics*, Vol. 86, No. 3, pp. 716–722, May 2013, https://doi.org/10.1007/s10891-013-0887-y

[3] Sunil Kumar Sachdeva and Praveen Ailawalia, "Plane strain deformation in thermoelastic microelongated solid," *Civil and Environmental Research*, Vol. 7, No. 2, pp. 92–98, 2015.

[4] P. Ailawalia, S. K. Sachdeva, and D. S. Pathania, "Plane strain deformation in a thermoelastic microelongated solid with internal heat source," *International Journal of Applied Mechanics and Engineering*, Vol. 20, No. 4, pp. 717–731, Dec. 2015, https://doi.org/10.1515/ijame-2015-0047

[5] P. Ailawalia, S. Kumar, and D. S. Pathania, "Internal heat source in thermoelastic microelongated solid under Green Lindsay theory," *Journal of Theoretical and Applied Mechanics*, Vol. 46, No. 2, pp. 65–82, Jun. 2016, https://doi.org/10.1515/jtam-2016-0011

[6] P. Ailawalia, S. K. Sachdeva, and D. S. Pathania, "A two dimensional problem on laser pulse heating in thermoelastic microelongated solid," *Archives of Thermodynamics*, Vol. 40, No. 2, pp. 69–85, 2019, https://doi.org/10.24425/ather.2019.129542

[7] P. Ailawalia and A. Singla, "A thermoelastic microelongated layer immersed in an infinite fluid and subjected to laser pulse heating," *Mechanics and Mechanical Engineering*, Vol. 23, No. 1, pp. 233–240, Jul. 2019, https://doi.org/10.2478/mme-2019-0031

[8] M. I. A. Othman, S. Y. Atwa, E. E. M. Eraki, and M. F. Ismail, "A thermoelastic micro-elongated layer under the effect of gravity in the context of the dual-phase lag model," *ZAMM – Journal of Applied Mathematics and Mechanics / Zeitschrift für Angewandte Mathematik und Mechanik*, Vol. 101, No. 12, Dec. 2021, https://doi.org/10.1002/zamm.202100109

[9] M. I. A. Othman, R. S. Tantawi, and E. E. M. Eraki, "Effect of rotation on a semiconducting medium with two-temperatures under L-S theory," *Archives of Thermodynamics*, Vol. 38, No. 2, pp. 101–122, Jun. 2017, https://doi.org/10.1515/aoter-2017-0012

[10] H. W. Lord and Y. Shulman, "A generalized dynamical theory of thermoelasticity," *Journal of the Mechanics and Physics of Solids*, Vol. 15, No. 5, pp. 299–309, Sep. 1967, https://doi.org/10.1016/0022-5096(67)90024-5

[11] M. Ezzat, M. Zakaria, O. Shaker, and F. Barakat, "State space formulation to viscoelastic fluid flow of magnetohydrodynamic free convection through a porous medium," *Acta Mechanica*, Vol. 119, No. 1-4, pp. 147–164, Mar. 1996, https://doi.org/10.1007/bf01274245

[12] M. A. Ezzat and A. A. El-Bary, "Memory-dependent derivatives theory of thermo-viscoelasticity involving two-temperature," *Journal of Mechanical Science and Technology*, Vol. 29, No. 10, pp. 4273–4279, Oct. 2015, https://doi.org/10.1007/s12206-015-0924-1

[13] M. A. Ezzat, A. S. El-Karamany, and A. A. El-Bary, "Modeling of memory-dependent derivative in generalized thermoelasticity," *The European Physical Journal Plus*, Vol. 131, No. 10, pp. 1–12, Oct. 2016, https://doi.org/10.1140/epjp/i2016-16372-3

[14] M. A. Ezzat and H. M. Youssef, "Stokes' first problem for an electro-conducting micropolar fluid with thermoelectric properties," *Canadian Journal of Physics*, Vol. 88, No. 1, pp. 35–48, Jan. 2010, https://doi.org/10.1139/p09-100

[15] A. E. Green and K. A. Lindsay, "Thermoelasticity," *Journal of Elasticity*, Vol. 2, No. 1, pp. 1–7, Mar. 1972, https://doi.org/10.1007/bf00045689

[16] M. N. O. Zis¸Ik and D. Y. Tzou, "On the Wave Theory in Heat Conduction," *Journal of Heat Transfer*, Vol. 116, No. 3, pp. 526–535, Aug. 1994, https://doi.org/10.1115/1.2910903

[17] D. Y. Tzou, "Experimental support for the lagging behavior in heat propagation," *Journal of Thermophysics and Heat Transfer*, Vol. 9, No. 4, pp. 686–693, Oct. 1995, https://doi.org/10.2514/3.725

[18] D. Y. Tzou, "A unified field approach for heat conduction from macro – to micro-scales," *Journal of Heat Transfer*, Vol. 117, No. 1, pp. 8–16, Feb. 1995, https://doi.org/10.1115/1.2822329

[19] A. M. Alharbi, E. M. Abd-Elaziz, and M. I. A. Othman, "Effect of temperature-dependent and internal heat source on a micropolar thermoelastic medium with voids under 3PHL model," *ZAMM – Journal of Applied Mathematics and Mechanics / Zeitschrift für Angewandte Mathematik und Mechanik*, Vol. 101, No. 6, pp. 1–24, Jun. 2021, https://doi.org/10.1002/zamm.202000185

[20] E. M. Abd-Elaziz and M. I. A. Othman, "Effect of Thomson and thermal loading due to laser pulse in a magneto-thermo-elastic porous medium with energy dissipation," *ZAMM – Journal of Applied Mathematics and Mechanics / Zeitschrift für Angewandte Mathematik und Mechanik*, Vol. 99, No. 8, Aug. 2019, https://doi.org/10.1002/zamm.201900079

[21] M. I. A. Othman and E. M. Abd-Elaziz, "The effect of thermal loading due to laser pulse in generalized thermoelastic medium with voids in dual phase lag model," *Journal of Thermal Stresses*, Vol. 38, No. 9, pp. 1068–1082, Sep. 2015, https://doi.org/10.1080/01495739.2015.1073492

[22] P. Ailawalia and S. Budhiraja, "Dynamic problem in elastic solid using dual-phase-lag model with internal heat source," *Journal of Mathematical Sciences and Applications*, Vol. 2, No. 1, pp. 10–16, 2014, https://doi.org/10.12691/jmsa-2-1-3

[23] M. I. A. Othman, W. M. Hasona, and E. M. Abd-Elaziz, "Effect of rotation on micropolar generalized thermoelasticity with two temperatures using a dual-phase lag model," *Canadian Journal of Physics*, Vol. 92, No. 2, pp. 149–158, Feb. 2014, https://doi.org/10.1139/cjp-2013-0398

[24] M. I. A. Othman and E. M. Abd-Elaziz, "Dual-phase-lag model on micropolar thermoelastic rotating medium under the effect of thermal load due to laser pulse," *Indian Journal of Physics*, Vol. 94, No. 7, pp. 999–1008, Jul. 2020, https://doi.org/10.1007/s12648-019-01552-1

Appendix

A1.

$$a_1=\frac{\mu}{\rho c_1^2},\quad a_2=\frac{\lambda+\mu}{\rho c_1^2},\quad a_3=\frac{\beta_1\lambda_0 c_1^2}{a_0\beta_0 w^{*2}},\quad a_4=\frac{\lambda_1 c_1^2}{a_0 w^{*2}},\quad a_5=\frac{\lambda_0^2}{a_0\rho w^{*2}},$$
$$a_6=\frac{\rho j_0 c_1^2}{2a_0},\quad a_7=\frac{\rho c_e c_1^2}{kw^*},\quad a_8=\frac{\beta_0^2 T_0}{k\rho w^*},\quad a_9=\frac{\beta_1\beta_0 T_0 c_1^2}{k\lambda_0 w^*},$$
$$a_{10}=a_1+a_2,\quad a_{11}=\Omega^2-w^2-a_{10}b^2,\quad a_{12}=\Omega^2-w^2-a_1b^2,\quad a_{13}=a_5b^2,$$
$$a_{14}=b^2+a_4+a_6w^2,\quad a_{14}=b^2+a_4+a_6w^2,\quad a_{15}=\left(1+\tau_q w\right),$$
$$a_{16}=(1+\tau_\theta w),\quad a_{17}=a_8a_{15}w,\quad a_{18}=a_8a_{15}w\,b^2,\quad a_{19}=a_{16}b^2+a_7a_{15}w,$$
$$a_{20}=\frac{\lambda+2\mu}{\rho c_1^2},\quad a_{21}=\frac{\lambda}{\rho c_1^2},$$
$$A=\frac{1}{a_1a_{10}a_{16}}(a_1a_{17}-a_1a_5a_{16}-a_1a_{11}a_{16}+a_1a_{10}a_{19}-a_{10}a_{12}a_{16}+a_1a_{10}a_{14}a_{16}),$$
$$B=\frac{-1}{a_1a_{10}a_{16}}(-a_1a_{18}+a_{12}a_{17}-4a_{16}w^2\Omega^2+a_1a_{13}a_{17}+a_1a_5a_{19}+a_1a_{13}a_{16}+a_1a_{11}a_{19}$$
$$-a_1a_{14}a_{17}-a_5a_{12}a_{16}-a_{11}a_{12}a_{16}+a_{10}a_{12}a_{19}+a_1a_{11}a_{14}a_{16}-a_1a_{10}a_{14}a_{19}$$
$$+a_{10}a_{12}a_{14}a_{16}+a_1a_5a_9w-a_1a_3a_9a_{10}w),$$
$$C=\frac{1}{a_1a_{10}a_{16}}(-a_{12}a_{18}+4a_{19}w^2\Omega^2-a_1a_3a_{18}+a_3a_{12}a_{17}-a_1a_{13}a_{19}+a_1a_{14}a_{18}$$
$$+a_5a_{12}a_{19}+a_{12}a_{13}a_{16}+a_{11}a_{12}a_{19}-a_{12}a_{14}a_{17}+4a_{14}a_{16}w^2\Omega^2-a_1a_{11}a_{14}a_{19}$$
$$+a_{11}a_{12}a_{14}a_{16}-a_{10}a_{12}a_{14}a_{19}-a_1a_9a_{13}w+a_5a_9a_{12}w-a_1a_3a_9a_{11}w-a_3a_9a_{10}a_{12}w),$$

$$E = \frac{-1}{a_1 a_{10} a_{16}}(a_{12}a_{14}a_{18} - a_{12}a_{13}a_{19} - a_3 a_{12}a_{18} - 4a_3 a_9 \Omega^2 w^3 - 4a_{14}a_{19}\Omega^2 w^2 - a_{11}a_{12}a_{14}a_{19} - a_9 a_{12}a_{13}w - a_3 a_9 a_{11}a_{12}w),$$

$$H_{2n} = \frac{-\ a_{17}k_n^4 + (a_{18} + a_{14}a_{17} - a_5 a_9 w)k_n^2 + (a_9 a_{13}w - a_{14}a_{18})}{(a_{19} + a_{14}a_{16})k_n^2 - a_{16}k_n^4 - (a_{14}a_{19} + a_3 a_9)},$$

$$H_{3n} = \frac{a_5 k_n^2 - a_{13} - a_3 H_{2n}}{(k_n^2 - a_{14})}, \quad H_{1n} = \frac{2\Omega w}{a_1 k_n^2 + a_{12}},$$

$$H_{4n} = -\ b^2 a_{20} - iba_{20}k_n H_{1n} + a_{21}k_n^2 + iba_{21}k_n H_{1n} - H_{2n} + H_{3n},$$

$$H_{5n} = a_{20}k_n^2 + iba_{20}k_n H_{1n} - b^2 a_{21} - iba_{21}k_n H_{1n} - H_{2n} + H_{3n},$$

$$H_{6n} = -\ iba_1 k_n + a_1 k_n^2 H_{1n} - iba_1 k_n + a_1 b^2 H_{1n}.$$

A2.

$$l_1 = \frac{\lambda^e + 2\mu^e}{\rho^e c_1^{e2}}, \quad l_2 = \frac{\lambda^e + \mu^e}{\rho^2 c_1^{e2}}, \quad l_3 = \frac{\mu^e}{\rho^e c_1^{e2}}, \quad l_4 = \frac{\lambda^e}{\rho^e c_1^{e2}},$$

$$\delta_1 = b^2 l_1 + w^2, \quad \delta_2 = l_3 b^2 + w^2, \quad G = \frac{b^2 l_2^2 - \delta_1 l_1 - \delta_2 l_3}{l_1 l_3}, \quad N = \frac{\delta_1 \delta_2}{l_1 l_3},$$

$$L_{1n} = \frac{l_3 r_n^2 - \delta_1}{ibl_2 r_n}, \quad L_{1(n+2)} = \frac{l_3 r_n^2 - \delta_1}{-ibl_2 r_n}, \quad L_{2n} = ibl_1 - r_n l_4 L_{1n},$$

$$L_{2(n+2)} = ibl_1 + r_n l_4 L_{1(n+2)}, \quad L_{3n} = ibl_4 - l_1 r_n L_{1n}, \quad L_{3(n+2)} = ibl_4 - l_1 r_n L_{1(n+2)},$$

$$L_{4n} = ibl_3 L_{1n} - l_3 r_n, \quad L_{4(n+2)} = ibl_3 L_{1(n+2)} + l_3 r_n.$$

Mohamed I.A. Othman received Ph.D. degree in 1994, in applied mathematics in Zagazig University, Egypt. Now he works at Faculty of Science, Zagazig University, Zagazig, Egypt. His current research interests include the field of theory of thermo-elasticity. Theory of two-temperature generalized thermoelasticity, thermo-elastic diffusion, thermoelastic with voids, fiber-reinforced, micropolar thermoelastic medium, photothermal waves in a semiconducting medium, piezo-thermoelastic and generalized thermo-micro-stretch elastic solid. He is one of the world's top 2 % of scientists 2020 and 2021 (according to Stanford University).

Sarhan Atwa received Ph.D. degree in 2009, in applied mathematics in Zagazig University, Egypt. Now he works at Higher Institute of Engineering, Dep. of Eng. Math. and Physics, Shorouk Academy, Cairo, Egypt. His current research interests include applied mathematics, mathematical physics, engineering, and computation.

E. Eraki received Ph.D. degree in 2017, in applied mathematics in Zagazig University, Egypt. Now she works at Faculty of Science, Zagazig University, Zagazig, Egypt. Here current research interests include the field of theory of thermo-elasticity. Theory of two-temperature generalized thermoelasticity, thermo-elastic diffusion, thermoelastic with voids, photothermal waves in a semi-conducting medium, piezo-thermoelastic and generalized thermo-micro-stretch elastic solid.

Mohamed Ismail received M. Sc. degree in 2022, in applied mathematics in Zagazig University, Egypt. Now he works at Higher Institute of Engineering, Dep. of Eng. Math. and Physics, Shorouk Academy, Cairo, Egypt. His current research interests include applied mathematics, mathematical physics, thermoelastic diffusion, thermoelastic with voids engineering, and computation.